NUMERICAL APPROACH FOR PREDICTION OF AIRFLOW BEHAVIOR IN COFFEE BEAN MONOLAYERS DURING DRYING PROCESS

Jaime Daniel Bustos-Vanegas[1*], Larissa Aragón[1], Nelson Gutiérrez-Guzmán[1], Nancy Córdoba[1]

[1*]Corresponding author. Cesurcafé - Universidad Surcolombiana/ Neiva, Colombia.
E-mail: jaime.bustos@usco.edu.co | ORCID ID: https://orcid.org/0000-0002-1512-5143

KEYWORDS

coffee quality, porous medium, pressure drop, renewable energy, optimization, CFD.

ABSTRACT

The homogeneity and efficiency of moisture removal from coffee beans depend on the airflow patterns inside the drying chambers used for drying. This study aimed to implement a porous medium model to simulate the airflow through mesh trays containing parchment and ripe fruit coffee (*Coffea arabica* L.) using computational fluid dynamics (CFD). The geometry of the ripe fruit and parchment coffee beans was simplified as spherical and semi-ellipsoidal, respectively. The pressure drop in the normal direction to the monolayer was calculated as the average pressure of the normal planes located 1 mm before and after the bean layer for different air velocities. The viscous and inertial terms were adjusted by nonlinear regression for each case and incorporated into the Navier–Stokes equations as subdomains. The pressure drops calculated by the porous medium model and those calculated using the bean layers presented a good fit. The modeling of the trays as porous media can help reduce the computational resources required for CFD simulations while maintaining an acceptable accuracy.

INTRODUCTION

Over 100 species of coffee are known; among them only Arabica (*Coffea arabica* L.) and Robusta (*C. canephora*) are of economic importance. Arabica is preferred in the specialty coffee market owing to its complexity of aromas and flavors. In 2020, 10.1 billion kilograms of green coffee were produced in the world; 48.7% of this green coffee was produced in South America, 28.9% in Asia, 11.5% in Mexico and Central America, and 10.9% in Africa (ICO, 2020). Colombia has approximately 545,000 coffee growers, of which 95% have less than five hectares of land; thus, they are classified as small coffee growers (FNC, 2021). Drying is a critical stage in coffee production, which includes both wet (drying after the pulping and washing stages) and dry (ripe fruit or natural drying) processes (Henao et al., 2017). At this stage, the compounds that produce aroma must be preserved. As a result of processes to obtain a product that can be stored while preserving its physical, sensory, and innocuous quality, the bean moisture content is reduced from approximately 63% wb to the range of 10–12% wb. In Colombia, the traditional system for coffee drying has been open sun drying, a low-cost technique that has an inherent risk of decreasing the quality of the product owing to long processing times and exposure to environmental pollutants. Some producers use mechanical drying that incorporates fans and a fuel-burning system to maintain a constant temperature in a closed environment. This system minimizes the risk of quality deterioration and enables the processing of large volumes (Kulapichitr et al., 2019; Rotta et al., 2021). However, the method has limitations in terms of the installation and operation cost.

Solar energy can be utilized in drying chambers either directly (using translucent materials) or indirectly (using solar collectors). Buoyancy owing to the density gradients of air at different temperatures (natural convection) is the driving force in this type of dryer. Fans can be coupled to improve the airflow inside the chamber (active solar dryers). Several studies have been carried out to increase the efficiency of this technology and reduce the processing time while maintaining the quality of the dry product (Basumatary 2013; Lakshmi et al., 2019a, 2019b; Singh & Gaur, 2020; Jawad et al., 2020; Güler et al., 2020).

In solar dryers designed by the Centro Nacional de Investigaciones de Café (CENICAFÉ), direct and diffuse radiation and hot air are used, where 2 cm thick layers of coffee can be dried in 4–7 days (Ramírez et al., 2002; Oliveros et al., 2008, 2017). Manrique et al. (2020) employed photovoltaic panels and a coffee husk burner to develop a hybrid solar-biomass coffee bean drying system. The authors managed to reduce electricity consumption by 66% and operating costs by 80% while maintaining the quality of the dry coffee.

In solar dryers, moist beans are placed on perforated trays (mesh) through which air flows and moisture is removed. For the drying process of specialty coffee, the Coffee Quality Institute (CQI) recommends batches with tray loads of 12 and 6 kg/m² for washed parchment and natural coffee, respectively. These loads create a bean monolayer that exerts resistance to airflow, depending on the shape, size, and arrangement of the grains. This resistance influences the pressure and air velocity inside the drying chamber and affects the heat and mass transfer coefficients. Therefore, optimal location and orientation of the trays are essential to minimize the formation of stagnant fluid regions formed due to the low values of these coefficients. These regions decrease the performance of the dryer, extending the drying time and jeopardizing the quality and reliability of the coffee. Although the dynamics of the airflow through the grain beds have been extensively investigated (De Ville & Smith, 1996; Tavares, 2018; Goneli et al., 2020; Al-Yahya & Moghazi, 1998; Gornicki & Kaleta, 2015), the information regarding the analysis of airflow through monolayers of ripe fruit and washed parchment coffee beans is not clear. Airflow prediction inside the dry chambers is essential for simulation stage as it helps to identify and avoid regions with low velocity and low heat and mass transfer coefficients.

The estimation of the air flow patterns, along with the prediction of the temperature and moisture distribution inside the drying chambers, can be obtained through the computational fluid dynamics (CFD) analysis. In recent years, CFD has been used as a design and optimization tool for storage, aeration, and drying systems for agricultural products (Pereira et al., 2015; Malekjani & Jafari, 2018; Silva et al., 2019; De Melo Aguiar et al., 2019; Vélez-Piedrahita et al., 2019; Salvatierra-Rojas et al., 2021; Villagrán & Bojacá, 2019; Panigrahi et al., 2020, 2021). Most CFD software is based on the finite volume technique, which guarantees the conservation of transported properties owing to its formulation. The accuracy of this technique depends on the size and shape of the control volumes (mesh); the more refined the mesh, the higher the accuracy. The use of this tool is limited because complex geometries demand refined meshes and, consequently, high computational resources. In the case of dryers containing several trays of coffee beans, a high-quality mesh would require a large number of cells at a high computational cost. The method proposed in this study aims to simulate airflow resistance through the bean layers using a momentum source instead of the whole bean geometry (Bustos-Vanegas et al., 2019; Gautam et al., 2021). The implementation of this model will allow for the simulation of different configurations of solar dryers at a low computational cost using the CFD codes.

MATERIAL AND METHODS

The airflow through a monolayer of coffee beans, which was contained in a virtual wind tunnel, was modeled and simulated using CFD. This simulation employed the academic version of the ANSYS CFX 2021-R1 software (ANSYS Inc.). The geometry of the ripe fruit, washed parchment coffee, and wind tunnel were designed using the ANSYS Design Modeler software (ANSYS Inc.). Cherry coffee beans (ripe fruit) and parchment coffee beans were simplified as spherical and semi-ellipsoidal, respectively. The wind tunnel was configured to be 12 × 12 cm wide and 31 cm high. A monolayer of beans (cherry and parchment separately) was positioned 10 cm from the entrance of the tunnel (Figure 1).
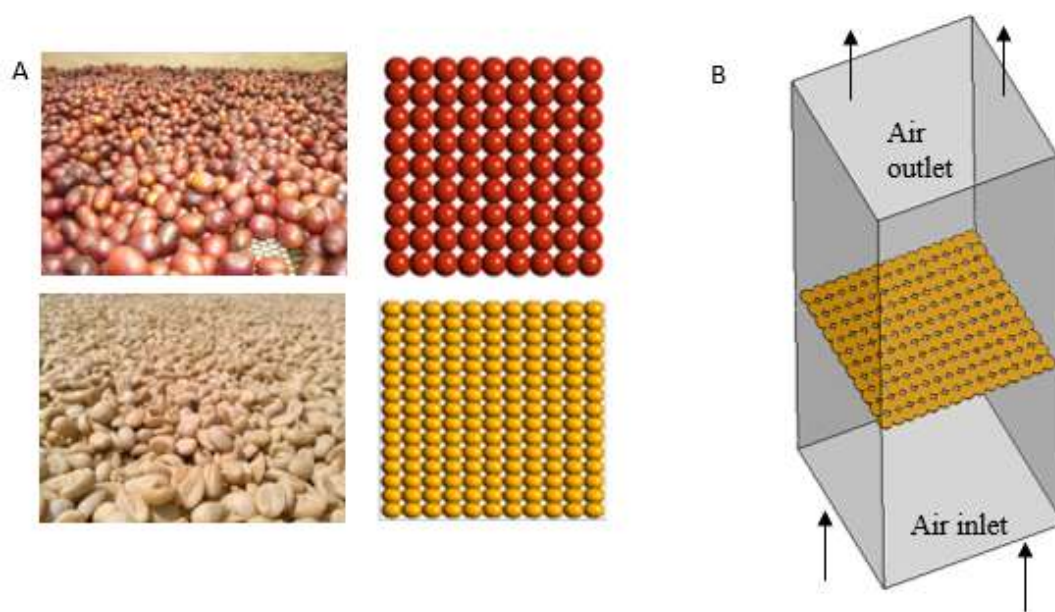

FIGURE 1. cherry coffee beans and washed parchment coffee on trays and its respective geometry (A) and computational domain for wind tunnel simulation (B).

The air inside the domain was treated as an ideal gas. Following the grid convergence analysis, an unstructured mesh with a maximum size of 0.005 m and refinement at the coffee beans' surface up to 0.003 m was defined so that a y+ value > 30 at the beans' surface could be established. The incompressible formulation of the Reynolds-averaged Navier–Stokes equations was solved using the CFX solver. Turbulence was modeled using the standard k–ε model (Pedras & Lemos, 2003; Saito & Lemos, 2010). The airflow direction in the solar dryers can be set from bottom to top owing to the buoyancy force resulting from the air density gradients. In the wind tunnel simulations, the inlet boundary condition was set to the normal air velocities—0.2, 0.5, 0.7, 1.0, and 1.5 m s^{-1}. The zero-pressure boundary condition was set at the outlet, and the symmetry condition was set at the walls. A no-slip wall boundary condition was set for the bean surfaces.

A high-resolution discretization scheme with second order accuracy was used for the advective term, and the residual target was set to a root mean square error (RMSE) value <10^{-6}. The pressure drop was calculated as the total pressure difference between the two planes located 1 mm above and below the bean layer. As described in [eq. (1)], the pressure drop in a flow through a porous medium is due to the resistance exerted by the viscous forces (first term on the right-hand side) and the resistance exerted by the inertial forces (second term on the right-hand side by momentum), which can be represented by linear and quadratic coefficients, respectively (Equation 2) (Bustos-Vanegas et al., 2019).

$$\frac{\Delta P}{l} = \left(\mu D + \frac{1}{2} F \rho |u| \right) u \qquad (1)$$

$$\frac{\Delta P}{l} = a \cdot u + b \cdot u^2 \qquad (2)$$

Where:

$\Delta P/l$ is the pressure drop per unit length, Pa m^{-1};

μ is the air dynamic viscosity, N s m^{-2};

D is viscous resistance, m^{-2};

F is inertial resistance, m^{-1};

ρ is air density, kg m^{-3}, and

u is the air inlet velocity, m s^{-1}.

The values of the parameters a and b were obtained for each process (ripe fruit and washed parchment coffee) using the non-linear regression (Equation 2) to fit the simulated pressure-drop data.

The porous medium model was implemented by replacing each bean monolayer with a subdomain (an equal-volume hexahedron) and adding the loss terms (parameters a and b) to the Navier–Stokes equation for each case. Simulations were performed in a virtual wind tunnel containing the subdomains, and the results were compared with the same simulations using the fully resolved, simplified coffee beans.

Finally, a porous-medium model was used to simulate the airflow inside a cabinet-type solar coffee dryer in its closed configuration (Figure 2B). In this case, the air enters through the lower lateral openings, crossing the mass of the coffee beans perpendicularly and exiting through the upper part of the dryer. A scenario implementing a possible upgrade using two coupled fans was also simulated. This dryer consists of a 1 × 1 m area and a 1.5 m high chamber with five trays 20 cm apart. Its mobile cover, made of high-density translucent polyethylene, allows direct exposure to the sun (Figure 2A) and retracts the trays on nights or rainy days (Figure 2B). The domain was discretized using a mesh of 1,12,500 hexahedral elements. The coffee bean layer in the mesh trays was modeled as a subdomain incorporating inertial and viscous forces (Table 1: cherry coffee beans) in the Navier–Stokes equation. To simulate the thermosiphon effect, the exit velocity at the top of the chamber was set to 0.5 m s^{-1}. The inlet boundary condition at atmospheric pressure was set at the bottom of the chamber. The fans were added as moment source terms (100 Pa m^{-1}) in the Navier–Stokes equation.
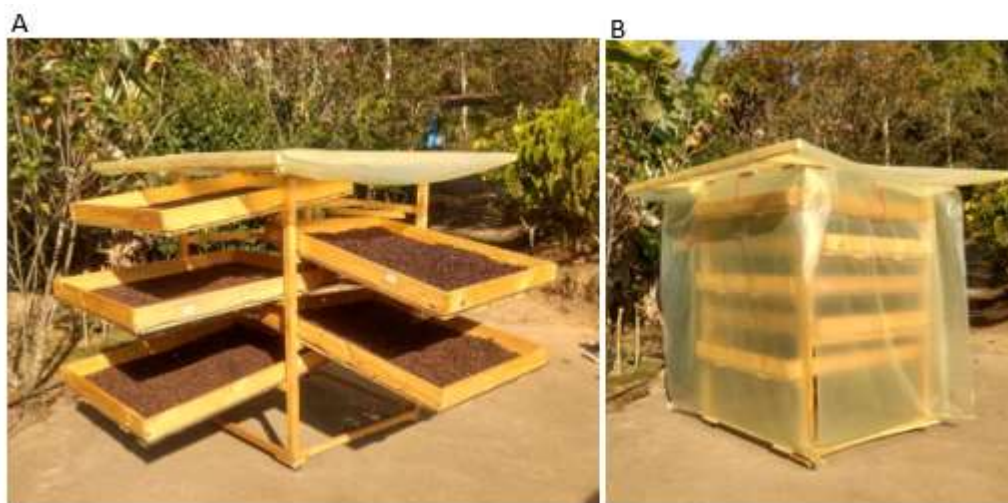

FIGURE 2. Prototype of coffee solar dryer: A) Open arrangement for the use of solar energy directly B) Closed arrangement for rainy or night periods.

RESULTS AND DISCUSSION

In Figure 3A, the velocity contour in the wind tunnel that contains the cherry coffee beans is illustrated. As expected, the airflow accelerated in the spaces between the beans, and a marked deceleration was observed immediately after the air passed the coffee beans. Figure 3B shows the pressure drop as a function of the air inlet velocity. There is a good fit ($R^2 = 99\%$) between the data obtained from the simulation and Eq. (1). For the air velocity ranging between 0.2 and 1.5 m s^{-1}, the pressure drop increases from 170 Pa m^{-1} to 6.364 Pa m^{-1} for washed

parchment coffee, and from 29 Pa m^{-1} to 1.560 Pa m^{-1} for ripe fruit. The calculated values for the pressure drop parameters were within the range reported in the literature. Altino & do Carmo Ferreira (2019) determined the pressure drop values varying between 400 and 2,500 Pa m^{-1} for airflow velocities between 0.2 and 0.6 m s^{-1} for soybean beds. Da Silva & Tavares (2018), using CFD, calculated the pressure drop for a washed parchment coffee layer with a thickness of 0.95 m. The authors used an airflow of 0.25 m s^{-1}, and determined an approximate pressure drop of 480 Pa m^{-1}.
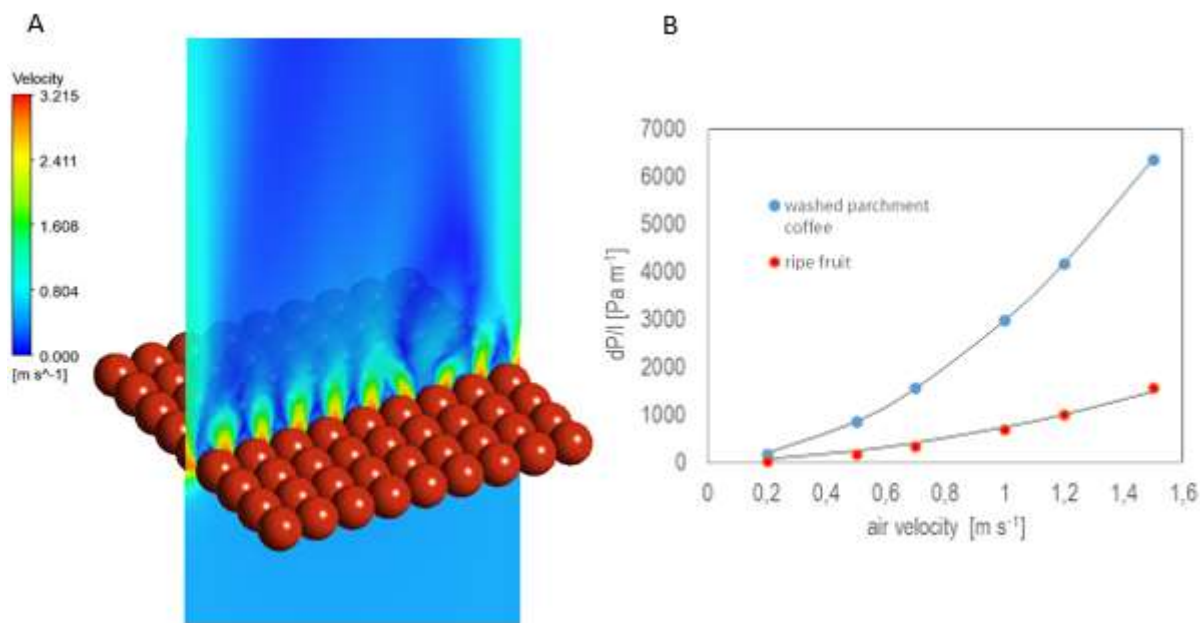

FIGURE 3. Flow patterns. A) velocity contour for cherry coffee beans with air inlet velocity of 0.5 m s^{-1}. B) Pressure drop as a function of air inlet velocity for cherry coffee beans and washed parchment coffee. Dots corresponds to CFD simulation. The line corresponds to values calculated by [eq. (1)].

Table 1 lists the values of the linear and quadratic coefficients (*a* and *b*) and viscous (D) and inertial (F) forces obtained by fitting Eq. (2) to the simulated data. The high pressure drop observed for the washed coffee is due to its geometry. Its flat side causes a marked fluid separation region, which increases the inertial forces. Viscous forces occur for both cherry and washed coffee, but, owing to the low dynamic viscosity of air, its contribution to the total pressure drop is minimal.

TABLE 1. Pressure drop parameters for airflow through monolayer of ripe fruit and washed parchment coffee.

Coffee process	*a* (kg m^{-3} s^{-1})	*D* (m^{-2})	*b* (kg m^{-4})	*F* (m^{-1})
Ripe fruit	250*	1.35E+07	500**	844.59
Washed	466**	2.52E+07	2516**	4250.95

**significant at 1% probability by t-test; *significant at 5% probability by t-test.

A significant decrease in the number of cells in the mesh generation was achieved by replacing the coffee bean geometry (502,359 elements) with porous subdomains (149,339 hexahedral elements). Consequently, the computational time was reduced by 90%. Figure 5 shows the pressure contours for a sample plane in the wind tunnel. As expected, the bodies of the beans caused fluid separation, and low-pressure regions could be observed behind the grain layer (Figure 4A). In the porous-medium approach, the pressure drop is a consequence of the addition of source terms to the momentum equation for each subdomain. Thus, the bean's boundary was eliminated, which inhibited fluid separation (Figure 4B). Although the local pressure differences between the two approaches were significant, the overall pressure drop was closed in both configurations—3.22 Pa for the bean geometry and 3.03 Pa for the porous medium. This proves the applicability of the porous medium approach.
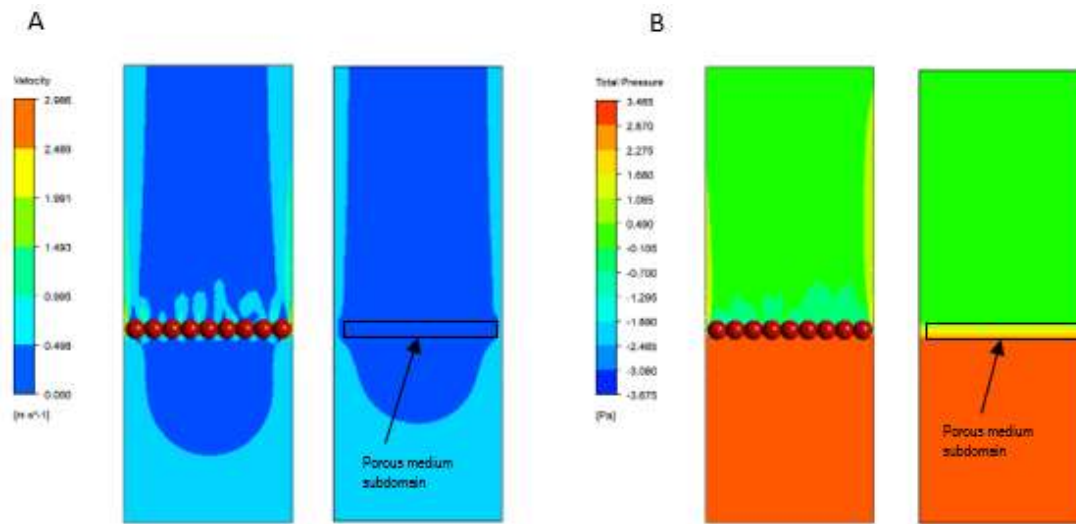
FIGURE 4. A) Velocity and B) pressure contours for airflow at 0.5 m s^{-1} through cherry coffee beans' geometry and porous medium model in wind tunnel.

Figure 5 presents the results of the simulation of airflow distribution inside the dryer presented in Figure 2B, loaded with 40 kg of cherry coffee beans distributed in five trays. The pressure drop in the central plane of the chamber is shown in Figure 5A. Low values of turbulent kinetic energy were observed in most of the chamber volumes (Figure 5B). This scenario leads to low heat and mass transfer coefficients, condensation, and long drying times, exposing the grains to undesirable microorganic (fungi) growth, mycotoxin development, and undesirable enzymatic reactions. The cup quality decreased eventually.
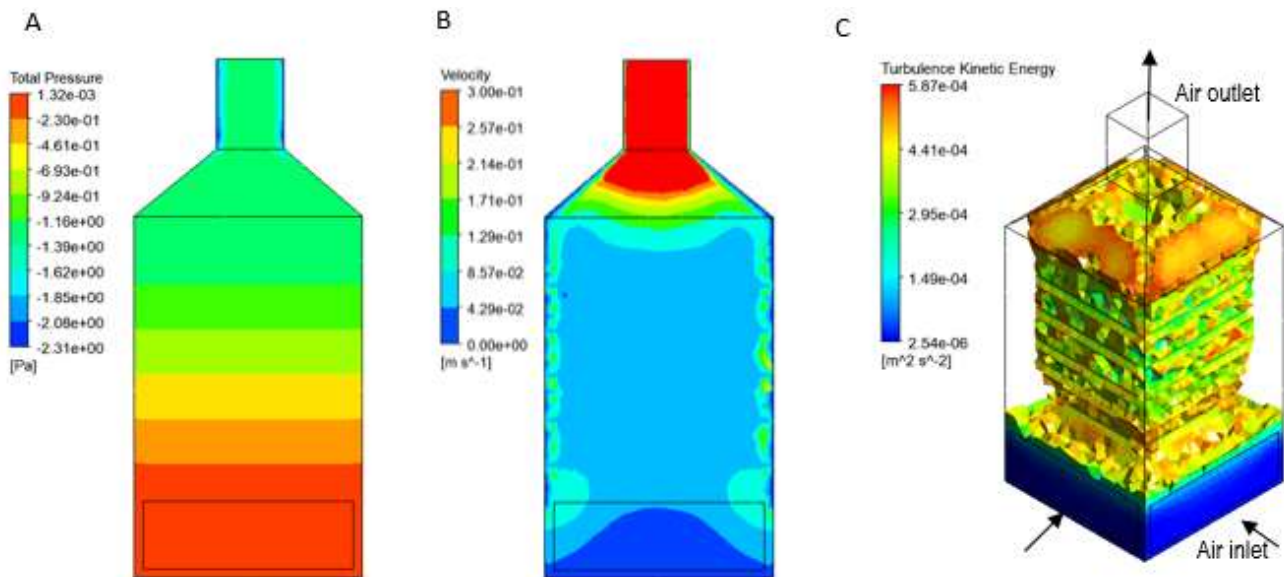

FIGURE 5. A) Pressure drop in a central plane. B) Modulus of velocity in a central plane. C) Turbulence kinetic energy values below 5.87e^{-4} J kg^{-1} in a solar dryer for coffee ripe fruit with porous medium model implemented.

The simulated scenario in Figure 5 leads to the formation of a layer of saturated air on the coffee bean surface. This slows or stops the drying process. In Figure 6, an alternative solution is proposed: the air movement caused by two fans over the first and third mesh trays considerably increases the turbulent kinetic energy (Figure 6A) and reduces the dead zones in most of the chamber volume (Figure 6B). The gray regions in Figure 7B (dead zones) represent the regions with air velocities less than 0.03 m s^{-1}. These regions correspond to 1.6% of the total effective volume of the drying chamber and are located mainly on the second and fifth mesh trays. This configuration was proposed as a low-cost alternative because it uses low-consumption fans (2.4 W) that can be driven by a small photovoltaic system.
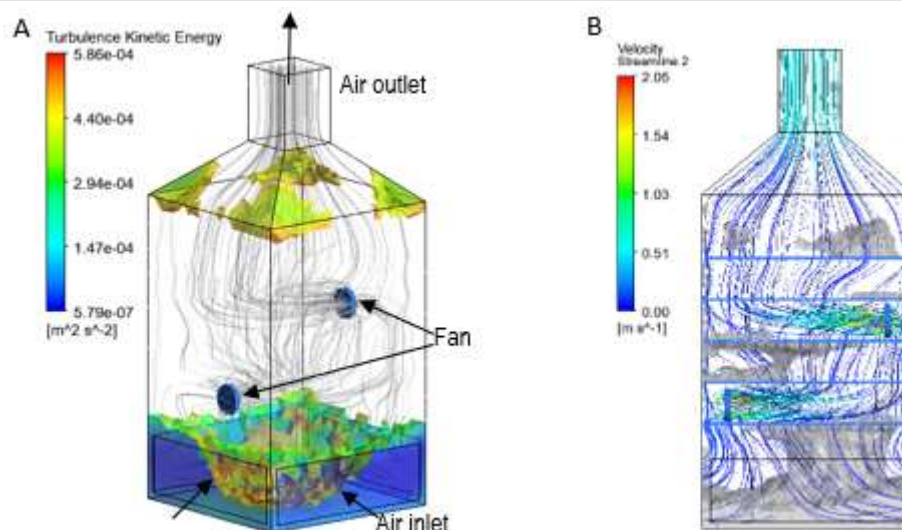
FIGURE 6. Active solar dryer for cherry coffee beans (porous medium model). A) turbulence kinetic energy values below 5.87e-4 J kg^{-1} and B) velocity streamlines. Gray regions represent velocity regions below 0.03 m s^{-1}.

Active solar dryers increase the airflow by coupling with mechanical ventilation. The different alternatives that have been implemented in the drying of agricultural products (Salvatierra-Rojas et al., 2021) and coffee (Manrique et al., 2020) may present advantages in terms of the reduction of processing time and disadvantages in terms of implementation and operation costs. With the implementation of low-energy-consumption fans, the simulated dryer in the final part of this study is presented as a possible solution to the specialty coffee drying problem.

CONCLUSIONS

A porous medium model was fitted and used to simulate the airflow resistance caused by mesh trays containing cherry coffee beans and washed parchment coffee in a monolayer arrangement. The model implementation allows the simulation of airflow into drying chambers containing several trays without incurring high computational costs. The implementation of the porous medium model is presented as a versatile tool for the design and optimization of drying chambers for specialty coffees using CFD. In future studies, the energy equation and moisture transport should be included in the mathematical model.

ACKNOWLEDGMENTS

REFERENCES

Al-Yahya SA, Moghazi HMM (1998) Static pressure drop through barley grain. Arab Gulf Journal of Scientific Research 16(1):223–239.

Altino HON, do Carmo FM (2019) Prediction of pressure drop through packed beds of granular materials: Influence of moisture reduction and air velocity. Brazilian Journal of Food Technology 22: 1–16. DOI: https://doi.org/10.1590/1981-6723.22818.

Basumatary B (2013) Design, Construction and Calibration of Low Cost Solar Cabinet Dryer. International Journal of Environmental Engineering and Management 4(4):351–358. Available: http://www.ripublication.com/ijeem.htm.

Bustos-Vanegas JD, Hempel S, Janke D, Doumbia M, Streng J and Amon T (2019) Numerical simulation of airflow in animal occupied zones in a dairy cattle building. Biosystems Engineering Elsevier Ltd 186:100–105. DOI: https://doi.org/10.1016/j.biosystemseng.2019.07.002.

CQI Coffee Quality Institute (2018) Course #2199: Q Processing Course Level 2 – Professional. Mayo 14 al 19 de 2018. Libro de trabajo del estudiante V 2.0.

Da Silva F, Tavares EA (2018) Static pressure drop across a bed of coffee beans: finite element analysis. Revista Ciencias Técnicas Agropecuarias 27(4):1–8.

De Melo Aguiar AC, Martins A, Barbosa RC, Bustos-Vanegas JD, Soares J, Olieira M, Rocha D, Gomes AF, Castro G (2019) Drying of microalga Scenedesmus obliquus BR003 in a gas dryer at low temperatures. Ciencia Rural 49(7):1–7. DOI: https://doi.org/10.1590/0103-8478cr20180928.

De Ville A, Smith EA (1996) Airflow through beds of cereal grains. Applied Mathematical Modelling 20(4):283–289. DOI: https://doi.org/10.1016/0307-904x(95)00121-y.

FNC - Federación Nacional de Cafeteros de Colombia (2021) Editorial. Ensayos sobre Economía Cafetera 34(1): 5-6.

Gautam KR, Rong L, Iqbal A, Zhang G (2021) Full-scale CFD simulation of commercial pig building and comparison with porous media approximation of animal occupied zone. Computers and Electronics in Agriculture (186):106206. DOI: https://doi.org/10.1016/j.compag.2021.106206.

Goneli ALD, Corrêa PC, Figueiredo A, Kirsch M, Botelho M (2020) Static pressure drop in layers of castor bean grains. Engenharia Agricola 40(2):184–191. DOI: https://doi.org/10.1590/1809-4430-ENG.AGRIC.V40N2P184-191/2020.

Gornicki K and Kaleta A (2015) Resistance of bulk grain to airflow – a review. Part I: Equations for airflow resistance. Annals of Warsaw University of Life Sciences - SGGW 65(65):31–41.

Güler HÖ, Sozen A, Dogus A, Afshari F, Khanlari A, Sirin C, Gungor A (2020) Experimental and CFD survey of indirect solar dryer modified with low-cost iron mesh. Solar Energy 197:371–384. DOI: https://doi.org/10.1016/j.solener.2020.01.021.

Henao CJD, Gutiérrez N, Orozco B (2017) Buenas prácticas y procedimientos para el secado de cafés especiales. Centro Surcolombiano de Investigación en Café - CESURCAFÉ. Pág.17

Jawad QA, Mahdy A, Khuder A, Chaichan M (2020) Improve the performance of a solar air heater by adding aluminum chip, paraffin wax, and nano-SiC. Case Studies in Thermal Engineering (19):100622. DOI: https://doi.org/10.1016/j.csite.2020.100622.

ICO (2020) International Coffee Organization - Historical Data on the Global Coffee Trade. Table 1: Crop Year Production by Country., 2020. Retrieved February 11, 2022, from International Coffee Orgainization website. Available: http://www.ico.org/prices/po-production.pdf.

Kulapichitr F, Borompichaichartkul C, Suppavorasatit I, Cadwallader K (2019) Impact of drying process on chemical composition and key aroma components of Arabica coffee. Food Chemistry (291): 49-58.

Lakshmi DVN, Muthukumar P, Layek A, Nayak P (2019a) Performance analyses of mixed mode forced convection solar dryer for drying of stevia leaves. Solar Energy (188):507–518. DOI: https://doi.org/10.1016/j.solener.2019.06.009.

Lakshmi DVN, Muthukumar P, Ekka J, Nayak P, Layek A (2019b) Performance comparison of mixed mode and indirect mode parallel flow forced convection solar driers for drying Curcuma zedoaria. Journal of Food Process Engineering 42(4). DOI: https://doi.org/10.1111/jfpe.13045.

Malekjani N, Jafari SM (2018) Simulation of food drying processes by Computational Fluid Dynamics (CFD); recent advances and approaches. Trends in Food Science and Technology (78):206–223. DOI: https://doi.org/10.1016/j.tifs.2018.06.006.

Manrique R, Vásquez D, Chejne F, Pinzón A (2020) Energy analysis of a proposed hybrid solar–biomass coffee bean drying system. Energy (202):1–8. DOI: https://doi.org/10.1016/j.energy.2020.117720.

Oliveros TCE, Ramírez GCA, Sanz UJR, Peñuela MAE (2008) Secador parabólico mejorado. Manizales, Cenicafé - Centro Nacional de Investigaciones de Café. Cenicafé. Avances Técnicos 376.

Oliveros TCE, Ramírez GCA, Tibaduiza VCA, Sanz UJR (2017) Construcción de secadores tipo túnel con nuevos materiales. Manizales, Cenicafé - Centro Nacional de Investigaciones de Café. Avances Técnicos 482.

Panigrahi S, Singh B, Fielke J (2020) CFD modelling of physical velocity and anisotropic resistance components in a peaked stored grain with aeration ducting systems. Computers and Electronics in Agriculture (179):105820

Panigrahi S, Singh B, Fielke J (2021) Strategies to mitigate dead-zones in on-farm stored grain silos fitted with aeration ducting modelled using computational fluid dynamics. Biosystems Engineering (205):93-104. DOI: https://doi.org/10.1016/j.biosystemseng.2021.02.013.

Pereira EMA, Silva JV, Andrade THF, Farias SR, Barbosa AG (2015) simulating heat and mass transfer in drying process: Applications in Grains. Diffusion Foundations (3):3–18. DOI: https://doi.org/10.4028/www.scientific.net/df.3.3.

Ramírez GCA, Oliveros TCE, Roa MG (2002) Construya el secador solar parabólico. Cenicafé - Centro Nacional de Investigaciones de Café. Avances Técnicos 305.

Rotta N, Curry S, Han J, Reconco R, Spang E, Ristenpart W, Donis-Gonzáles I (2021) A comprehensive analysis of operations and mass flows in postharvest processing of washed coffee. Resources, Conservation & Recycling (170):105554.

Salvatierra-Rojas A, Ramaj I, Romuli S, Muller J (2021) CFD-simulink modeling of the inflatable solar dryer for drying paddy rice. Applied Sciences 11(7). DOI: https://doi.org/10.3390/app11073118.

Silva MV, Martins MA, Faroni LR, Bustos-Vanegas JD, de Sousa H (2019) CFD modelling of diffusive-reactive transport of ozone gas in rice grains. Biosystems Engineering (179): 49–58. DOI: https://doi.org/10.1016/j.biosystemseng.2018.12.010.

Singh P, Gaur M K (2020) Review on development, recent advancement and applications of various types of solar dryers. Energy Sources, Part A: Recovery, Utilization and Environmental Effects. Taylor & Francis 00(00): 1–21. DOI: https://doi.org/10.1080/15567036.2020.1806951.

Vélez-Piedrahita S, Ciro-Velásquez H, Osorio-Saráz J, Largo-Avila E (2019) Estudio del efecto de la geometría de un secador solar típico para café con CFD. Revista Ingenierías Universidad de Medellín, 18(35): 149–161. DOI: https://doi.org/10.22395/rium.v18n35a9.

Villagrán EA, Bojacá CR (2019) Determination of the thermal behavior of a Colombian hanging greenhouse applying CFD simulation. Revista Ciencias Técnicas Agropecuarias 28(3):1–10.